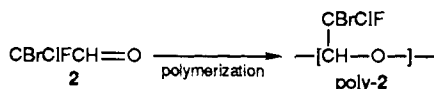


unit attached to the polyacetal main chain but also from the rigid helical polymer chain conformation which causes optical activity based on macromolecular asymmetry.<sup>6</sup>

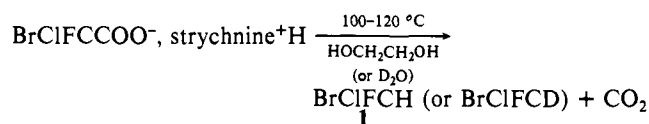


For the preparation of **2**, we started with 1-chloro-1,2,2-trifluoroethylene and obtained, after a sequence of five synthesis steps, bromochlorofluoroacetic acid (**3**) in about 25% yield.<sup>7</sup> **3** could be separated into the optical antipodes by fractional crystallization of its strychnine salt from methanol;<sup>1</sup> no melting point.

The determination of the optical purity was attempted by <sup>19</sup>F NMR spectroscopy of the strychnine salt of **3** in nonpolar solvents, but neither the salt nor the salt in the presence of shift reagents (chiral or achiral) gave satisfactory results. However, it was possible to determine the optical purity of **3** by esterification of the acid with borneol and employing <sup>19</sup>F NMR spectroscopy for the determination of the optical purity. The chemical shift of the diastereomeric esters gave fluorine shift values at about -63.8 ppm (relative to fluorotrichloromethane). The <sup>19</sup>F peaks of the diastereomers were separated by 0.13 ppm. The borneol ester of racemic **3** gave a 50/50 integration of the <sup>19</sup>F spectra for the diastereomers.<sup>7</sup>

The plot of the optical rotation as a function of optical purity of **3** (as determined by <sup>19</sup>F NMR spectroscopy of its borneol ester) resulted in a linear relationship. The pure antipode was calculated to have an  $[\alpha]^{22}_D$  of  $15.5 \pm 0.2^\circ$  (diethyl ether, 6.50 g/dL). The least soluble salt fraction yielded **3** with an  $[\alpha]^{22}_D$  of  $+10.3^\circ$  (diethyl ether, 6.86 g/dL) (path length 10 mm), and the most soluble salt fraction yielded **3** with an  $[\alpha]^{22}_D$  of  $-6.3^\circ$  (diethyl ether, 6.17 g/dL) (path length 10 mm). The enantiomeric excess was 66% (83/17 mixture of the (+) antipode) and 42% (29/71 mixture of the (-) antipode), respectively.

The strychnine salt of **3** was thermally decarboxylated in a heterogeneous medium between 100 and 120 °C when ethylene glycol or deuterium oxide was used as the decarboxylation medium; **1** was obtained in 50-70% yield in ethylene glycol and in 30% yield in deuterium oxide. Elemental anal. Calcd for CHBrClF: C, 8.15; H, 0.69. Found: C, 8.19; H, 0.70. NMR: <sup>1</sup>H, 7.35 and 7.95 ppm ( $J_{FH} = 54$  Hz); <sup>13</sup>C, 84.65 and 98.17 ppm ( $J_{FC} = 304.43$  Hz); <sup>19</sup>F, -80.09 and -80.74 ppm ( $J_{FH} = 54.99$  Hz).



The least soluble strychnine salt of (+)-**3** was decarboxylated in ethylene glycol, and **1** was obtained with an optical rotation of  $\alpha^{22}_D = +1.80 \pm 0.04^\circ$  (neat) (path length 1 dm). The most soluble strychnine salt of (-)-**3** after decarboxylation gave **1** with an optical rotation of  $\alpha^{22}_D = -0.92 \pm 0.04^\circ$  (neat) (path length 1 dm). When the extrapolated values of Collet<sup>5</sup> for optical purity ( $3.0 \pm 0.5^\circ$ ) were used, the optical purity of (+)-**1** was 60% and that of (-)-**1** was 31%. Using our determination of the optical purity of **3** by the borneol ester method<sup>7</sup> and assuming that no racemization had occurred during this decarboxylation procedure of **3** to **1**, we estimate a maximum value of  $\alpha^{22}_D$  of  $2.75 \pm 0.05^\circ$  as the value of the pure antipode of **1** (probably in the range of  $2.7^\circ$  and  $3.5^\circ$ ). This value is in good agreement with the value of  $\alpha^{22}_D = 3.0 \pm 0.5^\circ$  obtained previously.<sup>4,5</sup> The extrapolated value of ref 4 and 5 for optically pure **1** has the disadvantage of using **1** with a very low optical excess of the antipodes for the extrapolation.

We have also decarboxylated (-)-**3** (enantiomeric purity 34%) in deuterium oxide and obtained (-)-**1** with a deuterium purity (by <sup>19</sup>F spectroscopy) as high as 96%. The optical rotation of deuterated (-)-**1** was  $\alpha^{22}_D = -1.35 \pm 0.05^\circ$ ,  $\alpha^{22}_{365} = -2.35 \pm 0.05^\circ$  (neat, path length 2 mm), which corresponds to the optical rotation of deuterated **1** of  $\alpha^{22}_D = -4.0 \pm 0.3^\circ$  or  $\alpha^{22}_{365} = 7.0 \pm 0.5^\circ$  for 100% optical purity. NMR: <sup>13</sup>C, 81.72, 83.22, 84.72, 95.16, 96.66, and 98.17 ppm ( $J_{CF} = 302.97$  Hz and  $J_{CD} = 33.82$  Hz); <sup>19</sup>F, -82.09, -82.18, -82.31 ppm ( $J_{FD} = 8.3$  Hz).

Our results indicate that decarboxylations of the strychnine salts of **3** in protic (deuterio) media result in the formation of **1** with a high degree of selectivity in retention (or inversion) of the configuration. We believe that **1** of 100% optical purity could be obtained by decarboxylation of optically pure **3**; with our present accuracy limit, we can only predict an optical purity of at least 80%.

**Acknowledgment.** We thank J. Bartus for his assistance in the measurements of the optical rotations and his advice on experimental procedures, Paul Resnick, and Koichi Hatada and his research group for their assistance with the <sup>19</sup>F NMR spectroscopy of the borneol esters. We also appreciate the comments of Mark Green.

### Crystal Structure of Holoenolase Refined at 1.9 Å Resolution: Trigonal-Bipyramidal Geometry of the Cation Binding Site

Lukasz Lebioda\* and Boguslaw Stec<sup>†</sup>

Department of Chemistry  
University of South Carolina  
Columbia, South Carolina 29208  
Received July 24, 1989

We have determined and refined, using crystallographic restrained least squares, the structure of the enolase-Zn<sup>2+</sup> complex at 1.9-Å resolution. The final crystallographic *R* factor was 14.9%, and bond lengths in the molecule have a root-mean-square deviation from ideal values of 0.015 Å. The ligands of the Zn<sup>2+</sup> cation are all oxygen atoms which form an almost regular trigonal bipyramid with the monodentate carboxylic groups of Asp246 and Asp320 in the axial positions and the monodentate carboxylic group of Glu295 and two water molecules in the equatorial positions. The enolase-Zn<sup>2+</sup> complex has 80% of the activity of the physiological enolase-Mg<sup>2+</sup> complex,<sup>1,2</sup> so it is most probable that the Zn<sup>2+</sup> and Mg<sup>2+</sup> complexes are isostructural. The structure of the active ternary complex enolase-Mg<sup>2+</sup>-2-phosphoglycerate/phosphoenolpyruvate also shows a trigonal bipyramidal coordination geometry for Mg<sup>2+</sup> cation. A search through the Cambridge Crystallographic Database<sup>3</sup> did not find any all-oxygen trigonal-bipyramidal coordination geometry for Mg<sup>2+</sup> ion and only two for Zn<sup>2+</sup> ion. Thus the metal-ion environment in the active site of enolase is unusual and most probably critical for the catalytic process. It can be speculated that five-coordinated Mg<sup>2+</sup> or Zn<sup>2+</sup> ions are well suited for participation in enolase catalysis. They should strongly polarize the ligand, the H<sub>2</sub>O molecule or the hydroxyl group of 2-phosphoglycerate; on the other hand, the ion environment should be relatively unstable to allow easy dissociation of substrate/product molecules.

The structure of holoenolase is very similar to that of apo-enolase,<sup>4,5</sup> with an average deviation between the main-chain atoms of 0.19 Å and 0.31 Å between the side-chain atoms.

Enolase catalyzes the dehydration of 2-phospho-D-glycerate to phosphoenolpyruvate. All known enolases exhibit an absolute

(6) Corley, L. S.; Vogl, O. *Polym. Bull. (Berlin)* **1980**, *3*, 211-217. Doyle, T. R.; Vogl, O. *Polym. Bull. (Berlin)* **1985**, *14*, 535-540. Vogl, O.; Corley, L. S.; Harris, W. J.; Jaycox, G. D.; Zhang, J. *Makromol. Chem., Suppl.* **1985**, *13*, 1-12.

(7) Doyle, T. R. Ph.D. Dissertation, Polytechnic University, Brooklyn, NY 11201, 1989. Hatada, K.; Ute, K.; Nakano, T.; Okamoto, Y.; Doyle, T. R.; Vogl, O. *Polymer J. (Tokyo)* **1989**, *21*, 171-177.

<sup>†</sup> Permanent address: SLAFiBS, Jagiellonian University, Cracow, Poland.

(1) Wold, F.; Ballou, C. E. *J. Biol. Chem.* **1957**, *227*, 313.  
(2) Elliot, J. I.; Brewer, J. M. *J. Inorg. Biochem.* **1984**, *20*, 39.  
(3) Allen, F. H.; Kennard, O.; Taylor, R. *Acc. Chem. Res.* **1983**, *16*, 146. January 1989 edition of *Cambridge Structural Database*.  
(4) Lebioda, L.; Stec, B.; Brewer, J. M. *J. Biol. Chem.* **1989**, *264*, 3685.  
(5) Stec, B.; Lebioda, L. *J. Mol. Biol.* In press.

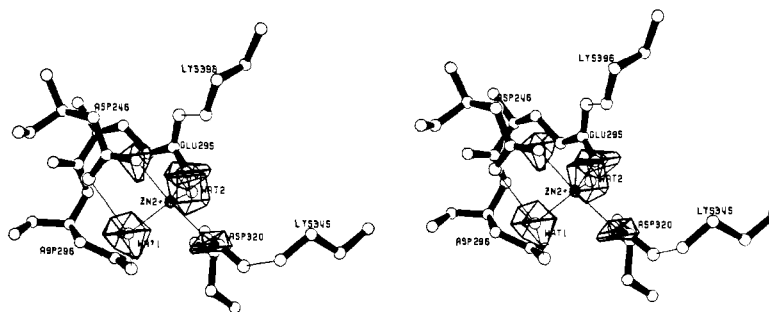


**Figure 1.** A stereoview of the metal-ion binding site of the enolase- $\text{Zn}^{2+}$  complex. The electron density, contoured at the  $6\sigma$  level, is from a  $F_o - F_c$  map calculated from a model in which the oxygen atoms coordinated to the  $\text{Zn}^{2+}$  ion were omitted. Abbreviations: Asp246 OD1, O1; Asp320 OD1, O2; Glu295 OE1, O3; WAT1, W1; and WAT2, W2. Bond lengths:  $\text{Zn}^{2+}$ -O1, 2.1 Å;  $\text{Zn}^{2+}$ -O2, 2.0 Å;  $\text{Zn}^{2+}$ -O3, 2.0 Å;  $\text{Zn}^{2+}$ -W1, 2.0 Å; and  $\text{Zn}^{2+}$ -W2, 2.3 Å. Angles: O1-Zn-O2, 172°; O3-Zn-W1, 120°; O3-Zn-W2, 120°; W1-Zn-W2, 120°; O1-Zn-O3, 92°; O1-Zn-W1, 90°; O1-Zn-W2, 81°; O2-Zn-O3, 90°; O2-Zn-W1, 96°; and O2-Zn-W2, 91°.

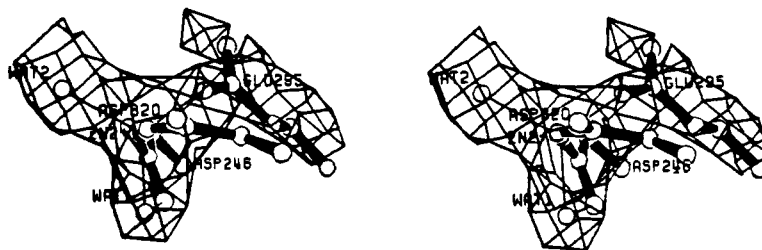


**Figure 2.** A stereoview of the metal binding site seen approximately along the axis of the bipyramid. The model displayed is of the enolase- $\text{Zn}^{2+}$  complex. The electron density, contoured at the  $1.7\sigma$  level, is from a Fourier map calculated with  $F_o - F_c$  coefficients, where the  $F_o$  are measured for the crystals of the ternary complex enolase- $\text{Mg}^{2+}$ -2-phosphoglycerate/phosphoenolpyruvate and the  $F_c$  are for the enolase- $\text{Zn}^{2+}$  complex model with the metal ion, the coordinated side chains, and the water molecules omitted. The map clearly indicates that the coordination of  $\text{Mg}^{2+}$  is similar to that of  $\text{Zn}^{2+}$ .

requirement for certain divalent cations for enzymatic activity, of which the natural cofactor  $\text{Mg}^{2+}$  gives the highest activity.<sup>6</sup> As isolated, the yeast enzyme contains endogenous tightly bound  $\text{Mg}^{2+}$ . The enzyme may be stripped of its endogenous  $\text{Mg}^{2+}$  and almost any other ion substituted. Metal-ion binding at this site is often<sup>6</sup> called "conformational". Not all conformational metal ions activate the enzyme, but there is no specificity for those that produce activity. Indeed,  $\text{Ca}^{2+}$ ,  $\text{Tb}^{3+}$ , and  $\text{Sm}^{3+}$ , which do not activate enolase, bind more tightly<sup>2</sup> than  $\text{Mg}^{2+}$ . It was proposed that the coordination of the activating conformational metal ion is octahedral and that the ligands are all oxy ligands, including two or three carboxyl groups and two water molecules.<sup>7</sup> A conformational metal ion must be present for substrate/product binding;<sup>8</sup> however, no catalysis occurs upon substrate binding. First, in the presence of substrate, additional metal-ion binding takes place although with much lower affinity. This additional metal ion is usually termed "catalytic". Higher than millimolar concentrations of activating metal ions actually inhibit enolase. The presence of an "inhibitory" binding site was postulated as one of the possible explanations of this effect.<sup>2</sup>

Crystals of enolase were obtained by the vapor diffusion method from solution containing 2% enolase, 2 mM  $\text{Mg}^{2+}$ , 1 mM EDTA, 1 mM dithiothreitol, 50 mM sodium citrate, pH = 5.0, and 27% saturated ammonium sulfate equilibrated against 55% saturated ammonium sulfate.<sup>9</sup> Crystals grown this way do not contain bound metal ions.<sup>4</sup> To study the holoenzyme structure, we transferred the crystals to a solution of 25 mM  $\text{Zn}^{2+}$ , 50 mM sodium citrate, pH = 6.0, and 70% saturated ammonium sulfate. The crystals did not show visible changes, and no loss of scattering power was observed. We have selected  $\text{Zn}^{2+}$  as the metal ion used because it gives the highest activity (80%) next to  $\text{Mg}^{2+}$ , it is much heavier than  $\text{Mg}^{2+}$  and, thus, has good contrast with  $\text{H}_2\text{O}$  molecules, and it binds more tightly than  $\text{Mg}^{2+}$ . Finally, we thought

that we would be able to determine the postulated inhibitory metal ion binding site.

Intensities, 59 713, were measured from one crystal and yielded in a merging and averaging procedure<sup>10</sup> 29 393 symmetry-independent reflections and  $R_{\text{int}} = 6.0\%$ . Reflections, 25 916 with  $F > 3\sigma(F)$ , in an 8–1.9-Å resolution range were used in the restrained least-squares refinement;<sup>11</sup> the starting model was that of apo-enolase<sup>5</sup> with the adjusted environment of  $\text{Zn}^{2+}$ .

The structure unequivocally shows 5-fold coordination for  $\text{Zn}^{2+}$ . An electron-density map phased by the model with the oxygen atoms coordinated to the metal ion omitted, presented in Figure 1, clearly indicates five ligands around  $\text{Zn}^{2+}$ . A similar arrangement of the ligands was found by us in the structure of enolase- $\text{Mg}^{2+}$ -substrate ternary complex,<sup>12</sup> see Figure 2.

The cation binding is accommodated by relatively very minor movements of the side chains. It appears that in the apo-enolase, at pH = 5.0, there is a proton located between the side chains of Glu295 and Asp320 and forming a short hydrogen bond;<sup>5</sup> the distance between the oxygen atoms is shortened from 2.8 Å in holoenolase to 2.6 Å in apo-enolase. The proton forming the H bond is thus partially replacing the metal-ion function.

The most unusual feature of holoenolase is the coordination of the metal ion, which is an almost regular trigonal bipyramid (Figure 1). A search through the Cambridge Crystallographic Database<sup>3</sup> for pentacoordinate  $\text{Zn}^{2+}$  ions with all oxygen ligands revealed two such ions with coordination geometries close to a square pyramid<sup>13</sup> and two in the coordination of a trigonal bipyramid.<sup>14</sup> A similar search for  $\text{Mg}^{2+}$  ions yielded only two

(10) Data collection was carried out at the Midwest Area Detector Facility by using a Nicolet diffractometer and the XGEN software.

(11) Hendrickson, W. A.; Konner, J. H. In *Biomolecular Structure, Function, Conformation and Evolution*; Srinivasan, R., Ed.; Pergamon Press: Oxford, 1980; p 43.

(12) Data, 2.2-Å resolution, collected for ternary complex enolase- $\text{Mg}^{2+}$ -2-phosphoglycerate/phosphoenolpyruvate confirm the location of the active site and the 5-fold coordination of  $\text{Mg}^{2+}$ . However, due to the averaging, in the crystal, of two or more stages of catalysis, a precise positioning of the substrates at this stage of refinement is not possible.

(13) Bis(benzoylacetonato)zinc monoethanolate. Belford, R. L.; Chasteen, N. D.; Hitchman, M. A.; Hon, P.-K.; Pflueger, C. E.; Paul, I. C. *Inorg. Chem.* **1969**, *8*, 1312. Monoaquobis(acetylacetonato)zinc. Montgomery, H.; Lin-gelfelter, E. C. *Acta Crystallogr.* **1963**, *16*, 748.

(6) Brewer, J. M. *CRC Crit. Rev. Biochem.* **1981**, *11*, 209.

(7) Nowak, T.; Mildvan, A. S.; Kenyon, G. L. *Biochemistry* **1973**, *12*, 1690.

(8) Faller, L. D.; Johnson, A. M. *Proc. Natl. Acad. Sci. U.S.A.* **1974**, *71*, 1083.

(9) Lebioda, L.; Brewer, J. M. *J. Mol. Biol.* **1984**, *180*, 213.

isomorphous structures of pentakis(trimethylphosphine oxide)-magnesium perchlorate<sup>15</sup> and pentakis(trimethylarsine oxide)-magnesium perchlorate.<sup>16</sup> They both have a square-pyramidal coordination geometry. Thus it appears that enolase represents the first known trigonal-bipyramidal environment of Mg<sup>2+</sup> ions. With the known propensity of Mg<sup>2+</sup> for octahedral coordination, it is interesting to analyze how 5-fold coordination is achieved. It seems that the carboxylic ligands form a relatively rigid frame with the side chains of Glu295 and Asp320 stabilized by ion pairs formed with Lys396 and Lys345, respectively (Figure 1), and Asp246 by a hydrogen bond to Ala248 N. In the equatorial plane, in addition to OE1 of Glu295, there are two water molecules: WAT1 and WAT2. It would seem that these waters could adjust their position and create room for an additional water molecule ligand. The clue to the stability of the observed structure is most probably two strong H bonds, both 2.6 Å long, formed by WAT1 to the carboxylic groups of Asp246 and Asp296. They force the Glu295 OE1-Zn<sup>2+</sup>-WAT1 angle of 120°, which leaves room for only one more oxygen atom in the equatorial plane. WAT1 has a very low temperature factor,  $B = 7 \text{ \AA}^2$ , and its position is conserved in apoenolase, and in the complexes of enolase with nonactivating metal ions Ca<sup>2+</sup> and Sm<sup>3+</sup> which have an octahedral coordination geometry.<sup>17</sup> The other water molecule ligand, WAT2, has a significantly higher temperature factor,  $B = 22 \text{ \AA}^2$ . It is probably the H<sub>2</sub>O molecule that is replaced by the hydroxyl group of 2-phosphoglycerate in the forward reaction and that attacks C3 of the phosphoenolpyruvate molecule in the reverse reaction. The lower-resolution, 2.2-Å, studies of ternary complex enolase-Mg<sup>2+</sup>-2-phosphoglycerate suggest such a mechanism.<sup>12,17</sup>

In solution, where hexaquo complexes are the predominant form of Mg<sup>2+</sup> ions, substitution of inner-sphere water occurs<sup>18</sup> at a rate of  $10^{5.2} \text{ s}^{-1}$ . In enzymes with the same coordination geometry, the ligand substitution should be slower. Thus, for Mg<sup>2+</sup> enzymes, substrate dissociation could be the rate-limiting step. We propose that in enolase the unstable 5-fold coordination of the metal ion allows much faster ligand exchange than would be possible with the normal octahedral coordination.

In the structures of the Ca<sup>2+</sup> and Sm<sup>3+</sup> complexes of enolase, the metal-ion binding site is shifted 0.5 Å from the Zn<sup>2+</sup> binding site approximately toward WAT2. This shift and the larger ionic radii of the nonactivating metal ions create sufficient space at the metal ion to accommodate the third, additional water molecule. The resulting coordination is octahedral.

Despite the high concentration of Zn<sup>2+</sup> (25 mM), we did not find any evidence, in the final difference Fourier map, of metal-ion binding in the inhibitory site. It is possible that the inhibitory site is created only in the presence of substrate. We think so because at pH = 6.0 the crystals of yeast enolase survive soaking in 100 mM Mg<sup>2+</sup> and 20 mM 2-phosphoglycerate solution but shatter in 20 mM Zn<sup>2+</sup> and 20 mM 2-phosphoglycerate solution.

Overall, the structures of apo- and holoenolase in crystals seem to be almost identical, especially taking into account the pH and ionic strength differences.

The fact that we do not see conformational changes between apo- and holoenolase is probably due to the pH = 5.0 of studied apoenolase and the protonation of some of the metal carboxylic ligands. The conformational change observed upon divalent cation binding was reported at pH = 7.8.<sup>19</sup>

**Acknowledgment.** We thank Mary Deacon and Dr. Edwin M. Westbrook for help with the area detector data collection and Dr. J. M. Brewer for purified enolase. This work was supported by a grant from the National Institutes of Health (GM34994).

(14) Bis(acetylacetonato)zinc. Bennett, M. J.; Cotton, F. A.; Eiss, R. *Acta Crystallogr.* **1968**, *B24*, 904. Hydroxotris(2-chlorobenzoato)dizinc dihydrate. Nakacho, Y.; Misawa, T.; Fujiwara, T.; Wakahara, A.; Tomita, K. *Bull. Chem. Soc. Jpn.* **1976**, *49*, 595.

(15) Ng, Y. S.; Rodley, G. A.; Robinson, W. T. *Acta Crystallogr.* **1978**, *B34*, 2837.

(16) Ng, Y. S.; Rodley, G. A.; Robinson, W. T. *Inorg. Chem.* **1976**, *15*, 303.

(17) Lebioda, L.; Stec, B. In preparation.

(18) Frey, C. M.; Stuehr, J. *Met. Ions Biol. Syst.* **1974**, *1*, 51.

(19) Collins, K. M.; Brewer, J. M. *J. Inorg. Chem.* **1982**, *17*, 15.

## Ortho-Vinylation and Alkylation of Coordinated Triarylphosphines by Reaction of Olefins with Osmium Polyhydrides

Peter J. Desrosiers, Lisheng Cai, and Jack Halpern\*

Department of Chemistry, The University of Chicago  
Chicago, Illinois 60637

Received June 5, 1989

Although cyclometalation of coordinated arylphosphine ligands is a reaction of widespread occurrence, examples of directly observed functionalization of the resulting metal carbon bonds are still somewhat limited.<sup>1</sup> We report here a distinctive example of such a reaction involving the coupling of an olefin to the metal-bonded carbon atom of a cyclometalated triarylphosphine ligand to form a stable complex in which the resulting vinyl substituent is bonded to the metal.

Our studies relate to the reactions of OsH<sub>4</sub>L<sub>3</sub> and [OsH<sub>5</sub>L<sub>3</sub>]<sup>+</sup> (L = tri-*p*-tolylphosphine) depicted in the schemes. Treatment of a dichloromethane solution of OsH<sub>4</sub>L<sub>3</sub> with 1 equiv of HBF<sub>4</sub> at -78 °C yields the cationic pentahydride [OsH<sub>5</sub>L<sub>3</sub>]<sup>+</sup>, whose <sup>1</sup>H and <sup>31</sup>P NMR spectra<sup>2</sup> are similar to those of the known pentahydrides [OsH<sub>5</sub>(PPh<sub>3</sub>)<sub>3</sub>]<sup>+</sup><sup>3</sup> and [OsH<sub>5</sub>(PMe<sub>2</sub>Ph)<sub>3</sub>]<sup>+</sup>.<sup>4</sup> The rapid displacement of H<sub>2</sub> by Br<sup>-</sup> and I<sup>-</sup> to form OsH<sub>3</sub>L<sub>3</sub>Br and OsH<sub>3</sub>L<sub>3</sub>I obeys pseudo-first-order kinetics, suggestive of rate-determining dissociation of H<sub>2</sub>. This is consistent with other observations that protonated polyhydrides lose H<sub>2</sub> more readily than their neutral precursors.<sup>5</sup> The rate constant for H<sub>2</sub> dissociation from [OsH<sub>5</sub>L<sub>3</sub>]<sup>+</sup> at -20 °C,  $5.8 \times 10^{-4} \text{ s}^{-1}$ , is more than 6 orders of magnitude greater than that from OsH<sub>4</sub>L<sub>3</sub>,  $2.4 \times 10^{-10} \text{ s}^{-1}$ .<sup>6</sup>

[OsH<sub>5</sub>L<sub>3</sub>]<sup>+</sup> reacts rapidly with excess ethylene at -20 °C to form the coordinately unsaturated complex [OsHL<sub>3</sub>(η<sup>2</sup>-C<sub>2</sub>H<sub>4</sub>)]<sup>+</sup> (**1**) and 2 mol of ethane in greater than 90% yield (<sup>1</sup>H NMR).<sup>7,8</sup> The rate constant,  $4.8 \times 10^{-4} \text{ s}^{-1}$ , independent of [C<sub>2</sub>H<sub>4</sub>], is consistent with rate-determining dissociation of H<sub>2</sub>. Above -20 °C, **1** is converted under C<sub>2</sub>H<sub>4</sub> to the orthometalated complex [OsL<sub>2</sub>{P(*p*-tolyl)<sub>2</sub>(*p*-CH<sub>3</sub>C<sub>6</sub>H<sub>3</sub>)}(η<sup>2</sup>-C<sub>2</sub>H<sub>4</sub>)]<sup>+</sup> (**2**), characterized by <sup>1</sup>H and <sup>31</sup>P NMR spectroscopy.<sup>7</sup> **1** and **2** are related to the neutral complexes OsH<sub>2</sub>L<sub>3</sub>(η<sup>2</sup>-C<sub>2</sub>H<sub>4</sub>) (**3**) and OsHL<sub>2</sub>{P(*p*-tolyl)<sub>2</sub>(*p*-CH<sub>3</sub>C<sub>6</sub>H<sub>3</sub>)}(η<sup>2</sup>-C<sub>2</sub>H<sub>4</sub>) (**4**) derived from the corresponding reactions of OsH<sub>4</sub>L<sub>3</sub> with excess ethylene. **3** and **4** were isolated as white crystals and characterized by NMR spectroscopy and elemental analyses.<sup>7</sup> Protonation of either **3** or **4** at -60 °C under ethylene results in immediate conversion to **1** (Scheme I).

(1) Bruce, M. I. *Angew. Chem., Int. Ed. Engl.* **1977**, *16*, 73-86 and references therein.

(2) NMR data for [OsH<sub>5</sub>L<sub>3</sub>]<sup>+</sup>BF<sub>4</sub><sup>-</sup>: <sup>1</sup>H (CDCl<sub>3</sub>, 25 °C) δ -5.85 (quart,  $J_{\text{HP}} = 4 \text{ Hz}$ , 5 H, MH);  $T_1$  (min) = 82 ms (500 MHz, -32 °C); <sup>31</sup>P{<sup>1</sup>H} δ 7.24 (s). The low  $T_1$  value suggests that this complex may have a "nonclassical" structure, possibly [L<sub>3</sub>Os(H<sub>2</sub>)H<sub>3</sub>]<sup>+</sup>. Such a formulation has been proposed by Hamilton and Crabtree for the related complex [(Ph<sub>3</sub>P)<sub>3</sub>OsH<sub>5</sub>]<sup>+</sup>.<sup>3</sup> Because of the uncertainty in the precise partitioning of hydrogens between terminal and η<sup>2</sup> ligands, we prefer to use the "generic" designation "OsH<sub>5</sub>L<sub>3</sub>". No particular structural formulation is intended.

(3) Hamilton, D. G.; Crabtree, R. H. *J. Am. Chem. Soc.* **1988**, *110*, 4126-4133.

(4) Burno, J. W.; Huffman, J. C.; Caulton, K. G. *J. Am. Chem. Soc.* **1984**, *106*, 1663-1669.

(5) (a) Lundquist, E. G.; Huffman, J. C.; Folting, K.; Caulton, K. G. *Angew. Chem., Int. Ed. Engl.* **1988**, *27*(9), 1165-1167. (b) Fontaine, X. L. R.; Fowles, E. H.; Shaw, B. L. *J. Chem. Soc., Chem. Commun.* **1988**, 482-483 and references therein.

(6) Deducing from the rates of the reaction OsH<sub>4</sub>L<sub>3</sub> + *t*-BuNC → OsH<sub>2</sub>L<sub>3</sub>(*t*-BuNC) + H<sub>2</sub> between 55 and 85 °C.  $\Delta H^\ddagger = 25.4 \text{ kcal/mol}$  and  $\Delta S^\ddagger = -2 \text{ cal/mol-K}$ .

(7) NMR, analytical, and mass spectral data are listed in the supplementary material.

(8) While the presence of coordinated dichloromethane or an agostic phenyl-hydrogen interaction cannot be excluded, it is noteworthy that neither changing the solvent from CD<sub>2</sub>Cl<sub>2</sub> to CDCl<sub>3</sub> nor changing the anion from BF<sub>4</sub><sup>-</sup> to CF<sub>3</sub>SO<sub>3</sub><sup>-</sup> affected the NMR spectrum of [OsHL<sub>3</sub>(C<sub>2</sub>H<sub>4</sub>)]<sup>+</sup> appreciably. The fact that both **1** and the orthometalated analogue, **2**, are intensely red-brown both in solution and in the solid state, whereas all the coordinately saturated osmium complexes that we have prepared are colorless or pale yellow, also supports the coordinately unsaturated formulation.